Electronic Supplementary Information for:

Membrane Curvature Recognition by C-Reactive Protein Using Lipoprotein Mimics

Min S. Wang, Reid E. Messersmith and Scott M. Reed*

Department of Chemistry, University of Colorado Denver, Denver, CO 80217

***Corresponding Author:**

Scott M. Reed

Department of Chemistry

University of Colorado Denver

Denver, CO 80217-3364

Phone: 303-556-6260

Fax: 303-556-4776

Email: scott.reed@ucdenver.edu

Supplementary Methods

Dynamic Light Scattering

The size distribution of AuNPs and LPP mimics was determined using dynamic light scattering (DLS, Malvern Zetasizer Nano N90s). An aliquot of sample (400 μL) was placed in a cuvette (1.5 mL, VWR) and illuminated at a fixed 90° angle with a He-Ne laser (633 nm). Each measurement was repeated 3 times and reported as mean intensity distribution ± SD.

UV-vis Measurements

Absorbance spectrum of the AuNPs were measured using a Perkin Elmer Lambda 650 spectrophotometer. A 1 mL solution of AuNPs was added to a cuvette and the absorbance was measured from 800-400 nm with 2 nm resolution and slit width of 2 mm.

Characterization of LPP mimics

AuNPs of various sizes (∅ 9-56 nm) were prepared using Fren's method [1] by varying the amounts of citrate in the solution (Table S1). The average sizes of the AuNPs were determined by DLS and AFM, and the diameters were in good agreement using either technique (Table S1). The completeness of lipid packing around the AuNP core was determined by cyanide stability test as previously described [2]. A complete lipid bilayer will protect the AuNP core from cyanide etching, while partially coated AuNP will be oxidized by cyanide and result in a reduction of the localized surface plasmon resonance (LSPR) (Table S2). UV/vis spectra of the LPP mimics obtained before and after 24 h of cyanide exposure showed stability for the LPP mimics as no significant decrease in absorbance (Δ AU < 5%) was observed after 24 h of exposure to cyanide (supplemental Table 2). In addition, the stability of the LPP mimics were further

confirmed using an in-gel cyanide stability test after electrophoresis (Table S2). A time-course study revealed that the LPP mimics were cyanide-resistant for up to 1 h, while the uncoated AuNPs decomposed within 15 min (supplemental movie).

Supplementary Tables

Table S1. Synthesis and characterization of AuNPs. AuNPs of different sizes were synthesized by adding 250 μL $HAuCl_4$ to 100 mL DI water and varying the amounts of citrate (340 mM stock). AuNP diameter was determined using DLS and AFM. The concentration of each AuNP was determined by Beer's law using the absorbance at λ_{max} and the calculated extinction coefficients (ε) as previously described [3]. [a]Mean particle diameters were obtained from three DLS measurements. [b]Mean particle diameters were calculated form 62-97 randomly selected particles on 3 separate AFM images.

Citrate vol added (μL)	DLS ± SD[a] (nm)	AFM ± SD[b] (nm)	λ_{max} (nm)	ε ($M^{-1}cm^{-1}$)	Conc (M)
735	10.0 ± 1.6	10.1 ± 2.2 (*n* = 74)	515	1.06×10^{8}	4.21×10^{-12}
368	15.2 ± 0.6	16.5 ± 2.3 (*n* = 97)	515	4.78×10^{8}	2.83×10^{-12}
294	21.8 ± 0.8	20.0 ± 2.0 (*n* = 62)	518	1.18×10^{9}	6.20×10^{-13}
150	33.2 ± 0.9	30.4 ± 3.9 (*n* = 85)	525	4.77×10^{9}	1.93×10^{-13}
65	57.3 ± 0.8	55.0 ± 6.9 (*n* = 83)	531	3.14×10^{10}	1.98×10^{-14}

Table S2. Stability of LPP mimics by cyanide etching. Mean LPP diameters were determined from 3 DLS measurements ± SD. The stability of the LPP mimics was determined by measuring the absorbance of the LPPs before and after 24 h of cyanide exposure. LPP stability is indicated by ΔAU at λ_{max} of < 5%.

LPP mimic (nm)	λ_{max} (nm)	Abs as prepared (AU)	Abs 24 h post cyanide (AU)	ΔAU (%)
21.4 ± 2.7	525	0.349	0.345	-1
25.8 ± 4.6	528	0.491	0.499	1
28.3 ± 1.3	530	0.615	0.629	2
41.0 ± 6.9	536	0.542	0.547	1
64.4 ± 2.4	540	0.397	0.406	2

Supplementary Figures

Figure S1. Binding of CRP to LPP mimics by gel electrophoresis. LPP mimics, with (+) and without (-) CRP were electrophoresed on an 0.5 X TBE, 0.8% agarose gel with 0.005% SDS at 40V for 30 min. (i) A digital photograph of the gel was taken after electrophoresis, and the position of the LPP mimics is observable by the characteristic reddish-pink color LSPR band of the AuNPs. (ii) The position of CRP was determined by Western blot after electrophoresis. The same gel was transblotted onto nitrocellulose membrane and CRP was detected using a polyclonal anti-CRP antibody. Unbound CRP does not travel far from the wells (top of gel), whereas LPP mimic-bound CRP co-migrates with the LPP mimic (bottom of gel). (iii) The photograph of the gel and Western blot was superimposed to show the overlapping bands of the LPP mimic and CRP. LPP mimic-bound CRP has overlapping bands on the gel photograph and Western blot at the same position, while unbound CRP does not have any overlapping bands.

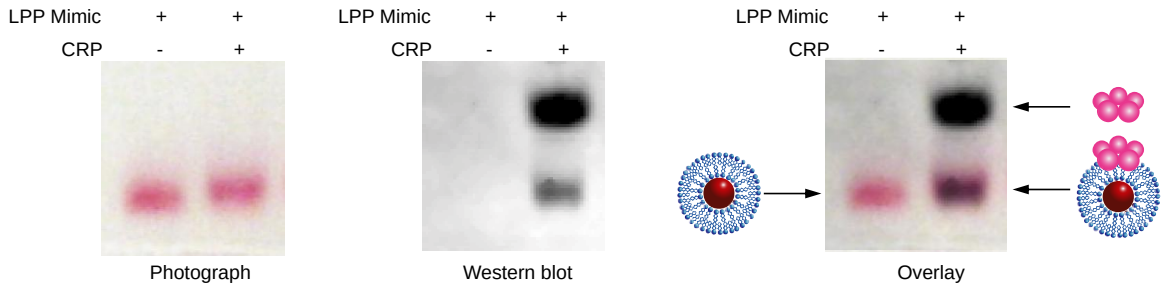

Figure S2. CRP isoform in the supernatant and pellet fractions. After 30 min incubation of CRP with LPP mimics in the presence of 250 μM $CaCl_2$, the mixture was centrifuged at 21,000 g for 30 min to pellet the LPP mimics. The supernatant (s) and pellet (p) fractions were also separated by gel electrophoresis (0.5 X TBE, 0.8% agarose with 0.005% SDS) and Western blot was used to confirm the prescence of CRP in each fraction. The Western blot showed significant amounts of mCRP in both fractions for the 21 nm LPP mimic. The amounts of mCRP in the supernatant decreased with increasing LPP mimic size; which was also accompanied by increased amounts of pCRP in the supernatant. Since the PC liposomes cannot be pelleted at 21,000 g, this sample contains only the supernatant and it was mostly pCRP. It is important to note that not all the supernatant can be successfully removed without disturbing the pellet; therefore trace amounts of supernatant remain in the pellet fraction.

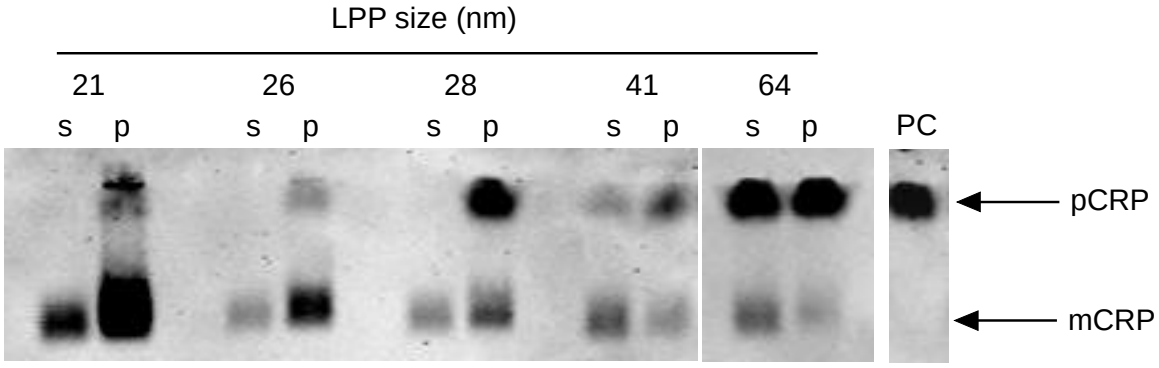

Figure S3. Schematic illustration of expected changes in fluorescence anisotropy when C1q binds to either an attached or soluble mCRP. Cy3 has a fundamental anisotropy of 0.386 and a 0.18 ns lifetime in PBS, making it well-suited for measuring rotational diffusion of marcomolesules.[4] CRP was pre-incubated with LPP mimics in the presence of 250 μM $CaCl_2$. Then, the 5'Cy3-RNA probe was added to the CRP-LPP mimic solution and baseline anisotropy was taken for 5 min. At the indicated time point (arrow), an aliquot of C1q was added to the CRP-LPP mimic-5'Cy3-RNA, incubated for another 15 min before the change in anisotropy (Δr) was measured. Because C1q only binds mCRP and the 5'Cy3-RNA only binds mCRP, target bound RNA probe will have a slower rotation rate (i.e., higher anisotropy) than free RNA probe. However there are two possible scenarios in the anisotropy increases: 1) C1q binds to mCRP that is still attached to the LPP mimic, or 2) C1q binds to mCRP that is released from the LPP mimics. The measured Δr will be a weighted average of Δr_a and Δr_b. Therefore, higher Δr is expected for mimic attached mCRP (Δr_a) compared to soluble mCRP (Δr_b).

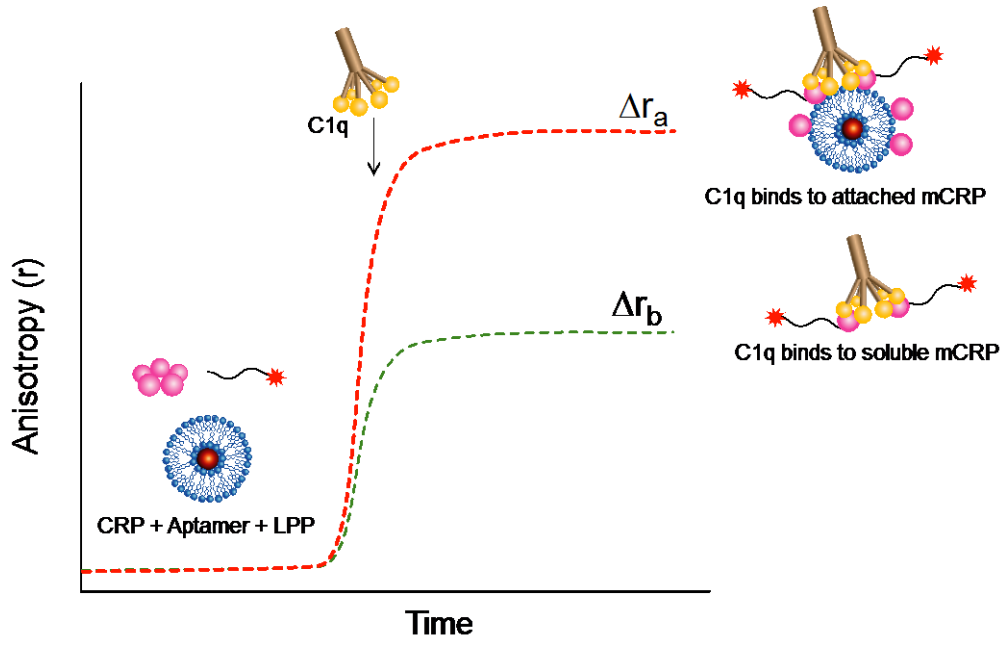

Figure S4. Diameters of small lipid vesicles (SLVs). SLVs were obtained by probe sonication, extrusion and templating around AuNP. Dried phosphatidylcholine (PC) lipid thin films (500 nmoles) were rehydrated with 1 mM HEPES buffer (1 mL, pH 6.5) followed by: extrusion through polycarbonate membranes (Avanti Polar Lipids); probe sonicated (Sonics Vibra Cell, VCX 130, CT) over ice water (1 sec on/2 sec off, 80% power, 20 min sonication time), or prepared using a AuNP template as described in this work. Diameters of SLVs were measured by DLS 30 min after SLV formation. An average of 3 DLS measurements were taken for each sample and the particle size was reported as % intensity. The probe sonicated SLVs (—**)** contained liposomes sizes between 30nm and 1 μm (PDI = 0.42). The 50-nm membrane pore extruded SLVs (—) have diameters of ~100 nm (PDI = 0.028); while the AuNP-templated SLVs (—) yielded the expected 25 nm (PDI = 0.24). PDI = polydispersity index.

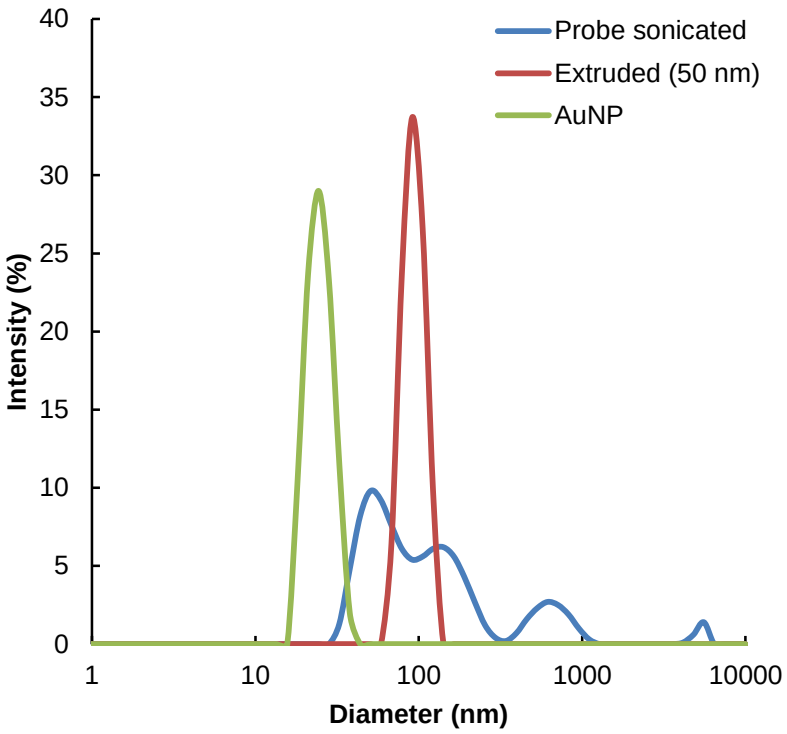

Figure S5. Curvatures of LPP mimics. (A) Mathematically, membrane curvature can be described by the two principle curvatures, C_1 and C_2, where the two perpendicular planes to the surface intercept[5]. The principle curvature is defined as $C_i = 1/R_i$, where R is the radius of the membrane[5], and the total curvature, $J = C_1+C_2$ [5]. Schematic illustrations of the (B-F) LPP mimics and (G) PC liposomes (drawn to scale) demonstrating curvature of the AuNP templates and possible lipid packing around the AuNPs. The phospholipids are shown in blue and AuNPs are in red. Note the larger LPP mimics (> 28 nm) and PC liposomes are geometrically flatter and less curved compared to the smaller LPP mimics (≤ 28 nm).

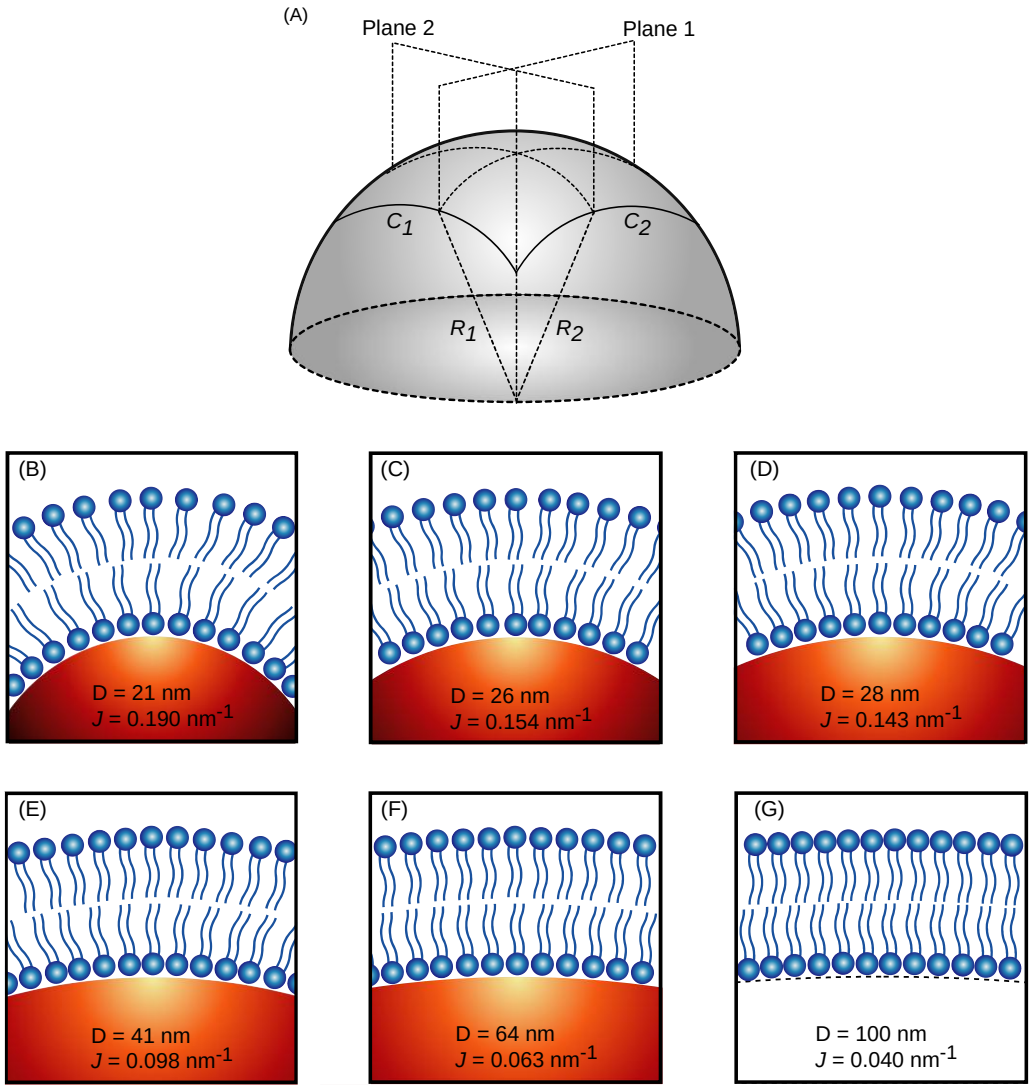

Figure S6. Oxidation of LDL samples monitored by (A) conjugated dienes [6] and by (B) electrophoretic mobility [7]. Oxidation of LDL (5.7 μg protein/mL) was induced by either air oxidation (air oxLDL) for 12 h at 37°C or by treatment with 4 μM $CuCl_2$ (CuLDL), followed by extensive dialysis against 1 X PBS. Conjugated dienes of the LDL samples were measured at 234 nm and the data was plotted as mean ± SD from three independent experiments. Electrophoretic mobilities of the LDL samples were determined by loading an aliquot of the sample on a 0.5%, 0.5 X TBE agarose gel that was pre-treated with SYTO 60 (1:50,000), an IR dye that intercalates with proteins and nucleic acid. Electrophoresis was carried out at a constant 70 V for 30 min and protein bands were visualized on an Odyssey IR imager using the 700 nm channel. Lanes: (1) native LDL from one gel and, (2) air oxLDL and (3) CuLDL run on a subsequent gel under the same conditions.

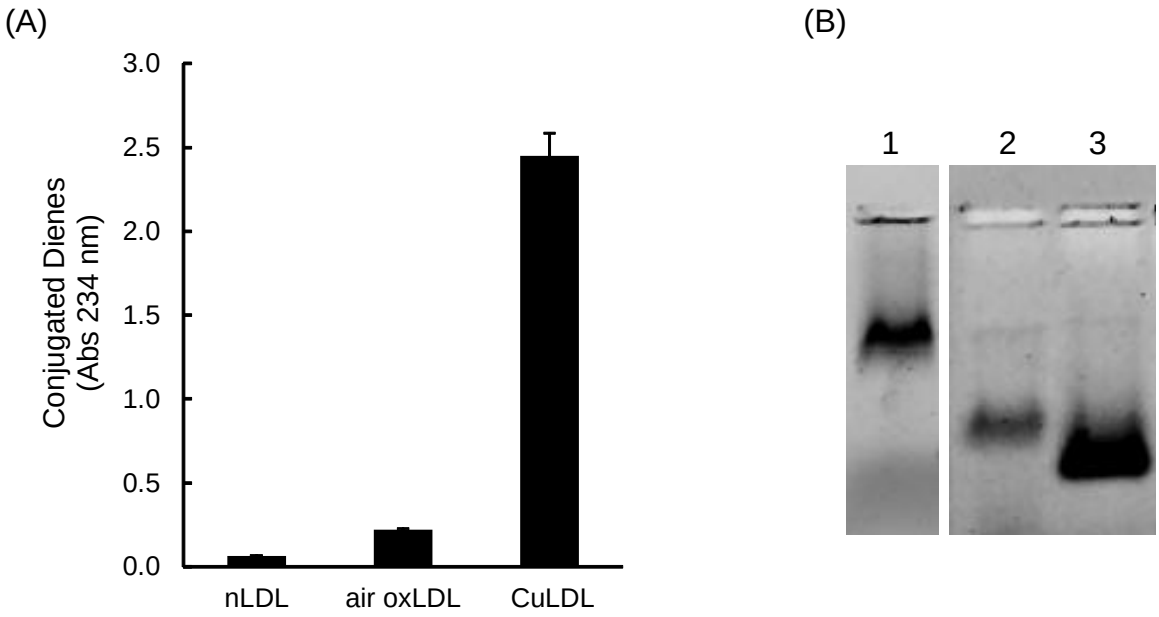

Supplemental References

1. S. Basu, S. Pande, S. Jana, S. Bolisetty and T. Pal, *Langmuir*, 2008, **24**, 5562-5568.
2. S. Sitaula, M. R. Mackiewicz and S. M. Reed, *Chem Commun*, 2008, 3013-3015.
3. X. O. Liu, M. Atwater, J. H. Wang and Q. Huo, *Colloid Surface B*, 2007, **58**, 3-7.
4. M. E. Sanborn, B. K. Connolly, K. Gurunathan and M. Levitus, *J Phys Chem B*, 2007, **111**, 11064-11074.
5. J. Zimmerberg and M. M. Kozlov, *Nature Reviews Molecular Cell Biology*, 2006, **7**, 9-19.
6. F. Martin-Nizard, C. Furman, P. Delerive, A. Kandoussi, J. C. Fruchart, B. Staels and P. Duriez, *J Cardiovasc Pharmacol*, 2002, **40**, 822-831.
7. D. L. Sparks and M. C. Phillips, *J Lipid Res*, 1992, **33**, 123-130.